Design of a Backstepping-Controlled Boost Converter for MPPT in PV Chains

Conference Paper · November 2019

DOI: 10.1109/ICAEE47123.2019.9014748

4 authors:

Okba Boutebba
Ferhat Abbas University of Setif
3 PUBLICATIONS **0** CITATIONS
SEE PROFILE

Samia Semcheddine
Ferhat Abbas University of Setif
13 PUBLICATIONS **10** CITATIONS
SEE PROFILE

Fateh Krim
Ferhat Abbas University of Setif
97 PUBLICATIONS **1,596** CITATIONS
SEE PROFILE

Billel Talbi
Ferhat Abbas University of Setif
23 PUBLICATIONS **98** CITATIONS
SEE PROFILE

Design of a Backstepping-Controlled Boost Converter for MPPT in PV Chains

Okba Boutebba, Samia Semcheddine, Fateh Krim, and Billel Talbi
Power electronics and industrial control laboratory (*LEPCI*), Department of electronics, Faculty of technology,
University of Sétif-1, 19000, Sétif, Algeria
boutebbaokba@gmail.com, tssamia@yahoo.fr, krim_f@ieee.org, bilel_ei@live.fr

***Abstract*—The objective of this work is to integrate the backstepping control for tracking the maximum power point of a photovoltaic (PV) chain. This control strategy is applied for a parallel DC-DC converter (type: boost) in order to regulate the output voltage of the PV generator, according to the reference voltage generated by the known perturb and observe (P&O) MPPT (maximum power point tracking) algorithm. The robust and nonlinear backstepping controller is based on Lyapunov function for ensuring the local stability of the system. The basic idea of the nonlinear backstepping controller *(BSC)* is to synthesize a control law in a recursive way, that is to say step by step. This controller has a good transition response, a low tracking error, and a very fast response to the changes in solar irradiation and environmental temperature. To prove the effectiveness of the suggested control method, a comparative study through numerical simulations is presented with sliding mode control (*SMC*) and the classical *PI* (proportional-integral) controller.**

Keywords*— *Boost converter; backstepping control; robustnes maximum power point tracking (MPPT); photovoltaic chain

I. INTRODUCTION

In recent years, a very important development of renewable energies has occurred because they have many advantages when compared to fossil fuels. With its inexhaustible potential and no negative impact on the environment [1], renewable energy is an appropriate and accessible technology for economic growth and sustainable development [2]. The study of the renewable energy conversion chain: primary energy extraction, electrical conversion, power generation, network transformation, and integration, is a basic element to improve the quality of production of "green" energy.

Given the current interest of the world in renewable energy in general and solar energy especially, photovoltaic (PV) panels are used today in plenty of applications. The PV array has a single operating point that can supply maximum power to the load. This point is named the maximum power point (MPP). The locus of this point has a nonlinear variation with temperature and solar radiation. Thus, in order to work the PV array at the MPP, the PV chain must include a maximum power point tracking (MPPT controller)

The boost type DC-DC converter is used generally in the PV chain as adaptation stage [3, 4]. This latter is connected to the output of the PV array and controlled by MPPT (Maximum power point tracking) algorithm in order to achieve the optimal voltage or current for harnessing the maximum PV energy.

Numerous MPPT methods have been developed and documented in the literature such as perturb and observe (P&O) [5-7], incremental conductance [2, 7-8], predictive-model-based approaches [9-11], sliding mode control-based MPPT (***SMC***) [12-15], fuzzy and artificial neural network methods [16-18].

In this paper, a robust nonlinear backstepping controller, which controls the duty cycle of a boost converter, is suggested. The output voltage of the PV array is the variable to be controlled; the output reference voltage of the PV array is delivered by a P&O algorithm to reach the MPP speedily. Consequently, the robustness is increased and Lyapunov's law ensures the global asymptotic stability and MPP is achieved even any environmental conditions.

This paper is structured as follows: in the second section description of PV chain, PV panel and boost k; modeling are introduced. In the third section, the backstepping control is detailed. Section ***IV*** *and* ***V,*** depict respectively analysis of the simulation results and comparison with SMC and *PI* controller and finally the conclusion.

II. DESCRIPTION OF PHOTOVOLTAIC CHAIN

The configuration of the PV chain under studied is given in Fig. 1. It represents a stand-alone structure composed of:

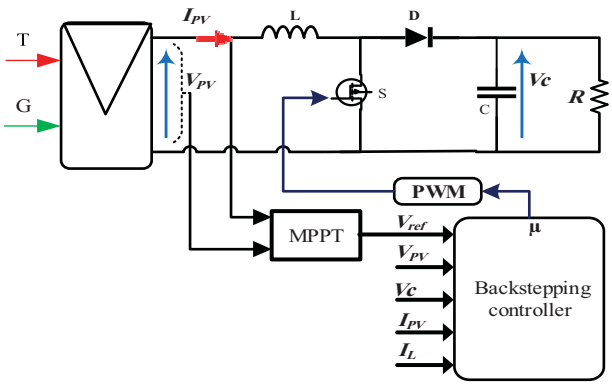

Fig. 1. Photovoltaic chain

978-1-7281-2220-5/19/$31.00 ©2019 IEEE.

- PV array which produces electrical energy directly from solar radiation.
- DC-DC boost converter with resistive load controlled by backstepping controller to release the MPPT operation. The backstepping controller block is the most important part of the system because it guarantees the necessary energy to the load.

A. PV panel modeling

The PV panel considered in this work is ***SIEMENS SM 110-24***, which is simulated using the model proposed in [18]. This model comprises a current generator in parallel with, series and shunt resistances R_s and R_{sh} Respectively.

The equations below are used to calculate the current generated by the PV panel :

$$I_{PV} = I_{Ph} - I_0\left[\exp\left(\frac{V_{PV} + Rs.I_{PV}}{\alpha.Vt}\right) - 1\right] - \left(\frac{V_{PV} + Rs.I_{PV}}{R_{Sh}}\right) \quad (1)$$

$$I_{Ph} = \left(I_{PV\_n} + Ki.\Delta T\right)\frac{G}{G_n} \quad (2)$$

$$Vt = \frac{Ns.K.T}{q} \quad (3)$$

$$I_0 = \frac{I_{sc\_n} + K.\Delta T}{\exp\left(V_{oc\_n} + \frac{Kv.\Delta T}{\alpha.Vt}\right)} \quad (4)$$

with

$\Delta T = T - Tn$ (T and Tn are the actual and nominal temperature respectively). I_{PV_n} and G_n are respectively the current generated by the light and the solar irradiation under nominal conditions. Ki and Kv are the current and voltage coefficients respectively. V_{oc_n} and I_{sc_n} are respectively the open circuit voltage and short-circuit current of the panel at nominal temperature. I_0 is the dark saturation current. I_{ph} is the photo-generated current.V_t is the thermal voltage. Rs and Rsh are series and shunt resistances respectively. Ns is the number of series cells in a PV panel and α is the diode quality factor. K is Boltzmann's constant and q is is electrical charge.

The PV array is comprised of several PV panels connected in series and parallel. Therefore, regarding on the PV panel model given by the Eq. 3, the PV array model can be expressed as

$$I_{PV} = N_{pp}.I_{Ph} - N_{pp}.I_0\left[\exp\left(\frac{N_{ss}.V_{PV} + Rs.I_{PV}\left(\frac{N_{ss}}{N_{pp}}\right)}{\alpha.Vt.N_{ss}}\right) - 1\right] - \left(\frac{N_{ss}.V_{PV} + Rs.I_{PV}\left(\frac{N_{ss}}{Npp}\right)}{R_{Sh}\left(\frac{N_{ss}}{N_{pp}}\right)}\right) \quad (5)$$

where Npp and Nss are the numbers of PV panels that are connected in parallel and series respectively.

B. Boost chopper modeling

The Dc-Dc boost converter is applied to step-up a DC voltage [3, 13]. This latter is used to shift the PV output voltage (V_{PV}) to the desired ***Vmpp*** by changing the value of duty cycle. The principal electrical circuit diagram of the boost chopper is presented in Fig. 2. It consists of the main components: Input voltage (V_{PV}), Transistor switches (S), Inductor (L), Diodes (D_1 & D_2), Capacitor (C_1 & C_2), Load (R).

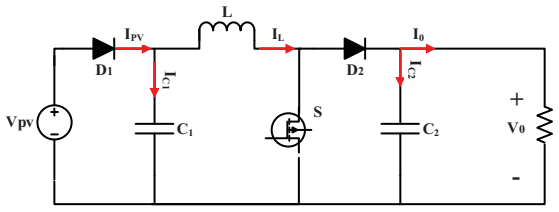

Fig. 2. Boost converter

It is assumed that the boost chopper is operating in ***CCM*** (the current I_L crossing the inductance ***L*** never get zero). There are two operating intervals of the converter, i.e. ***interval 1***, in which the switch is turned ***On***, and ***interval 2***, in which the switch is turned ***Off***.

- ***interval 1***, for the first period μTs: the IGBT switch (***S***) is ***ON***, the load ***R*** is disconnected due to the closed path by switch (***S***). Inductor (***L***) is charged from PV array through switch (***S)*** in this mode

Using Kirchhoff's voltage and current law, we can write

$$\begin{cases} Ic_1 = C_1\dfrac{dV_{PV}}{dt} = I_{PV} - I_L \\ Ic_2 = C_2\dfrac{dV_0}{dt} = -I_0 \\ V_L = L\dfrac{dI_L}{dt} = V_{PV} \end{cases} \quad (6)$$

- ***Interval 2***, for the second period $(1-\mu)Ts$: the switch (***S***) is turned ***OFF*** and the load ***R*** is connected directly to the inductor (***L***) via diode (***D2***).

Using kirchhoff's law, it yields

$$\begin{cases} Ic_1 = C_1\dfrac{dV_{PV}}{dt} = I_{PV} - I_L \\ Ic_2 = C_2\dfrac{dV_0}{dt} = I_L - I_0 \\ V_L = L\dfrac{dI_L}{dt} = V_{PV} - V_0 \end{cases} \quad (7)$$

To find a dynamic representation valid for all the period *Ts*, one generally uses the following averaging expression

$$\frac{dx}{dt}Ts = \frac{dx}{dt_{\mu Ts}}\mu Ts + \frac{dx}{dt_{(1-\mu)Ts}}(1-\mu)Ts \tag{8}$$

Applying the relation of Eq. 8 to the systems of Eqs. 6 and 7, we get the average model of the boost converter

$$\begin{cases} \dfrac{dV_{PV}}{dt} = \dfrac{I_{PV}}{C_1} - \dfrac{I_L}{C_1} \\ \dfrac{dV_0}{dt} = (1-\mu)\dfrac{I_L}{C_2} - \dfrac{I_0}{C_2} \\ \dfrac{dI_L}{dt} = \dfrac{V_{PV}}{L} - (1-\mu)\dfrac{V_0}{L} \end{cases} \tag{9}$$

$$\begin{cases} \dot{x}_1 = \dfrac{I_{PV}}{C_1} - \dfrac{x_2}{C_1} \\ \dot{x}_2 = \dfrac{x_1}{L} - (1-\mu)\dfrac{V_0}{L} \end{cases} \tag{10}$$

where $x = [x_1 \quad x_2]^T = [V_{PV} \quad I_L]^T$,represents the state vector and $\mu \in [0,1]$ is the duty cycles of the signal control.

III. BSC DESGIN

with a view to extracting the maximum energy from the PV array, a nonlinear controller ***BSC*** is aimed to track the PV array output tension ***VPV*** to ***Vmpp*** by controlling the duty cycle ***μ*** of the boost power converter. For this reason

Step 1:

First of all, we define the error signal

$$e_1 = V_{PV} - V_{ref} \tag{11}$$

where V_{ref} is the voltage reference produced by the P&O algorithm. By converging the e_1 to ($e_1 = 0$), we can acquire the desired result.

Using the Equation 10, the tracking error derivative is written as follows

$$\dot{e}_1 = \frac{I_{PV}}{C_1} - \frac{1}{C_1}x_2 - \dot{V}_{ref} \tag{12}$$

The following Lyapunov function is considered

$$V_1 = \frac{1}{2}e_1^2 \tag{13}$$

In order to ensure the asymptotic stability, this function of Lyapunov must be positive ($V_1 > 1$) definite and radially unbounded, and its derivative $\dot{V}_1$ with respect to time should be negative definite [19, 20]. Taking the time derivative of Eq. 13, we can get

$$\dot{V}_1 = e_1\dot{e}_1 \tag{14}$$

$$\dot{V}_1 = e_1\left(\frac{I_{PV}}{C_1} - \frac{1}{C_1}x_2 - \dot{V}_{ref}\right) \tag{15}$$

From this latter, the derivative of Lyapunov function to be negative, it is necessary to :

$$\frac{I_{PV}}{C_1} - \frac{1}{C_1}x_2 - \dot{V}_{ref} = -Ke_1 \tag{16}$$

From where

$$x_2 = C_1\left(K_1e_1 - \dot{V}_{ref}\right) + I_{PV} \tag{17}$$

Using the values of ***x2*** from Eq. 17, Eq. 15 becomes

$$\dot{V}_1 = e_1\left(\frac{I_{PV}}{C_1} - K_1e_1 + \dot{V}_{ref} - \frac{I_{PV}}{C_1} - \dot{V}_{ref}\right) \tag{18}$$

$$\dot{V}_1 = -K_1e_1^2 \tag{19}$$

Since the derivative of V_1 to be definitively negative, the value of K_1 must be defined positively, and Eq. 14 must be satisfied.

β : is the function of stabilization, acts as a reference current for ***x2***. then defined by

$$\beta = C_1\left(K_1e_1 - \dot{V}_{ref}\right) + I_{PV} \tag{20}$$

Hence the asymptotic stability of the system given by Eq. 10 in origin.

A. Step 2:

The 2nd error variable (e_2), which represents the difference between the state variable ***x2*** and its desired value β, is defined by

$$e_2 = x_2 - \beta \tag{21}$$

Or

$$x_2 = e_2 + \beta \tag{22}$$

Differentiating Eq. 22, Eq. 12 becomes

$$\dot{e}_1 = \frac{I_{PV}}{C_1} - \frac{1}{C_1}(e_2 + \beta) - \dot{V}_{ref} \tag{23}$$

$$\dot{e}_1 = -K_1e_1 - \frac{1}{C_1}e_2 \tag{24}$$

The derivative of ***e2*** can define as follows

$$\dot{e}_2 = \dot{x}_2 - \dot{\beta} \tag{25}$$

Therefore

$$\dot{e}_2 = \frac{1}{L}x_1 - \frac{1}{L}(1-\mu)V_0 - \dot{\beta} \quad (26)$$

In order to ensure the global asymptotic stability of the system and the convergence of the errors e_1 and e_2 to zero, a composite Lyapunov function V_t is defined whose time derivative must be negative definite for all values of $\boldsymbol{x_1}$ and $\boldsymbol{x_2}$.

$$V_t = V_1 + \frac{1}{2}e_2^2 \quad (27)$$

The derivative of V_t is

$$\dot{V}_t = \dot{V}_1 + e_2\dot{e}_2 \quad (28)$$

$$\dot{V}_t = -K_1 e_1^2 + e_2\left[-\frac{1}{C_1}e_1 + \frac{1}{L}\left(V_{PV} - (1-\mu)V_0\right) - \dot{\beta}\right] \quad (29)$$

For the derivative of V_t negative, it is necessary to

$$-\frac{1}{C_1}e_1 + \frac{1}{L}\left(V_{PV} - (1-\mu)V_0\right) - \dot{\beta} = -K_2 e_2 \quad (30)$$

From where

$$\mu = 1 - \frac{1}{V_0}\left[V_{PV} - L\dot{\beta} - L\left(\frac{1}{C_1}e_1 - K_2 e_2\right)\right] \quad (31)$$

IV. SIMULATION RESULTS

Firstly , numerical simulation of the PV chain shown in Fig. 1 is developed and implemented in MATLAB Simulink® environment. The photovoltaic array considered in this work consists of four identical PV panels shared into two parallel branches of two series connected panels. The parameters for the PV panel, the boost chopper and the ***BSC*** are indicated in Table 1.

TABLE I. PV MODULE , BOOST CHOPPER AND BSC CONTROLLER SPECIFICATIONS

	Parameters	***Values***
PV panel	Maximum power (Pmpp)	120 W
	Open circuit voltage (Voc)	42.1 V
	Short circuit current (Isc)	3.87 A
	Voltage at P_{Max} (Vmpp)	33.7 V
	Current at P_{Max} (Impp)	3.56 A
	Number of cells connected in series (Ns)	72
	Number of cells connected in parallel (Np)	1
Boost converter	Input capacitor C1	1100 µF
	Output capacitor C2	1100 µF
	Inductor L	1 mH
	Load R	50 Ω
Backstepping controller	K_1	500
	K_2	5000

A. Case 1: Test under varying levels of irradiance

Under this case, the temperature ***T*** is set constant at T= 25 °C and the irradiance ***G*** is subjected from time to time to a gradual change and a sudden change every 0.5 sec.

The profile of the different levels for irradiance is illustrated in Fig. 3. The profile starts at 400 W/m^2. During the first ascend (0.5 – 1 second), the irradiance increases gradually from 400 to1000 W/m^2.

Then, four consecutive step changes are made: (1000–600), (600–800), (800–600) and (600–1000) W/m^2. Finally, the level of irradiance descends gradually to primary state from 1000 to 400 W/m^2.

It can be seen from the results of simulations, during the variation of each irradiance level, that the proposed ***BSC*** tracks successfully the reference voltage ***Vref*** with less voltage fluctuations between (67.8- 68.2 V) has been recorded as shown in Fig. 4. The performance of the proposed controller is then confirmed.

Fig. 5 illustrated the obtained results of PV array with backstepping controller. It can be observed that the proposed controller has a very high performance at any level of irradiation and the controller performed well.

Fig. 6 shows the convergence of the error signal e_1 to zero below the sudden variation levels of irradiance at 1.5; 2; 2.5; 3 second and the gradual variation at 0.5; 4 seconds.

B. Case 2 :Test under varying levels of temperature

In this scenario, irradiance level is set constant at G=1000W/m^2 ,and temperature levels are varied.

The profile for the different levels of temperature is illustrated in Fig. 7. The profile starts at 25°C. During the first ascend (0.5 – 1 second), the irradiance increases gradually from 25 to 65°C.

Then, four consecutive step changes are made: (65–35), (35–45), (45–35) and (35–65) °C. Finally, the level of temperature descends gradually from 65 to 25 °C.

From photovoltaic array curves, the performance of the ***BSC*** is again confirmed, and good tracking to ***Vref***, as shown in Fig. 8. Thus, power $\boldsymbol{P_{PV}}$ achieves the P_{mpp} at the same time.

Moreover, one can deduce that the *BSC* presents a good transition response, and a very fast system reaction against set point change.

Fig. 10 shows the convergence of the error signal $\boldsymbol{e_1}$ to a null value under the variation of temperature at 1.5; 2.5; 3.5 second, with a low fluctuation between [-0.2, 0.2].

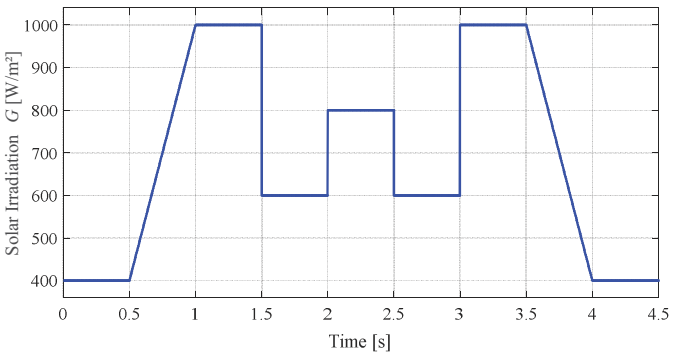

Fig. 3. Varying levels of irradiance

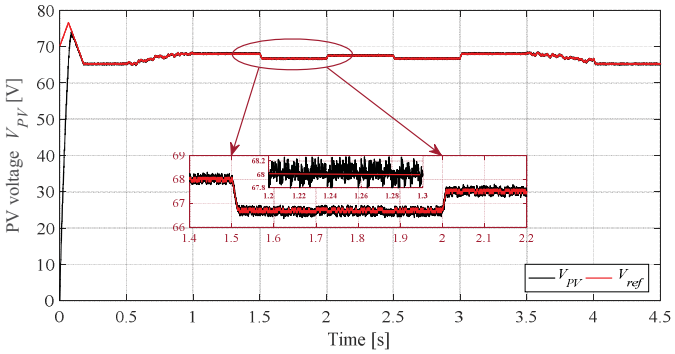

Fig. 4. Tracking of V_{PV} for different values of solar irradiation.

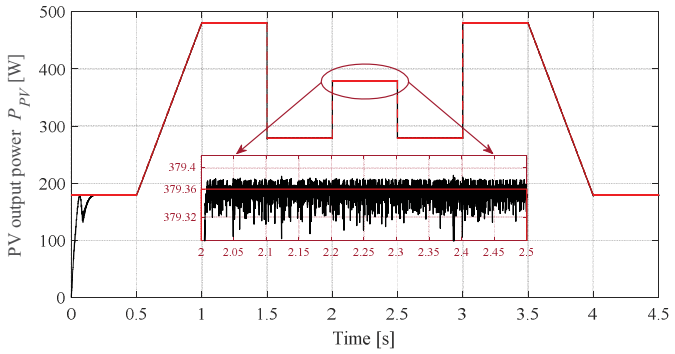

Fig. 5. Power of ***PV*** array for different values of solar irradiation.

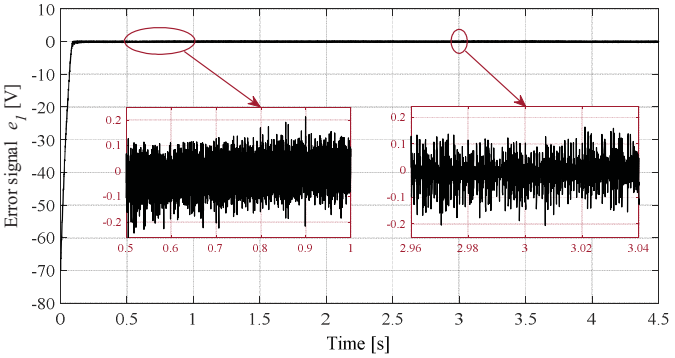

Fig. 6. Error signal e_1 under varying irradiance .

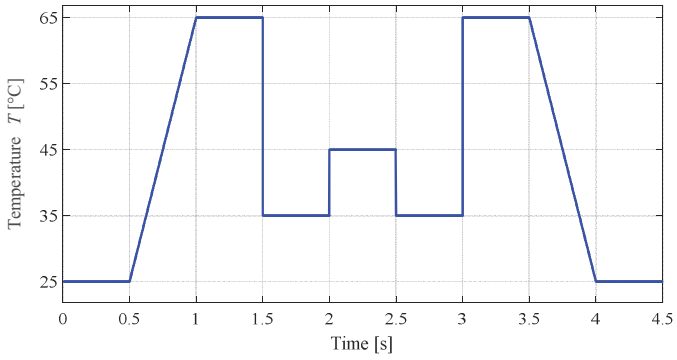

Fig. 7. Varying levels of temperature

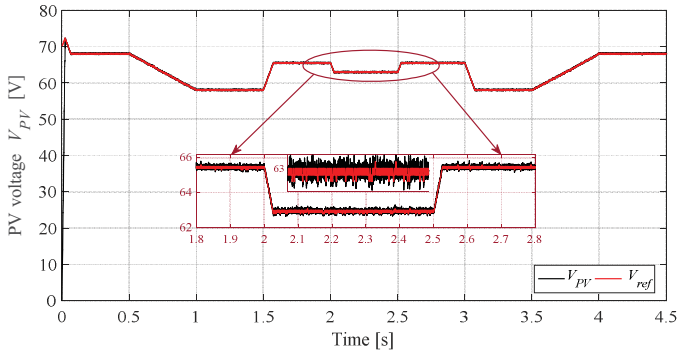

Fig. 8. Tracking of V_{PV} for different levels of temperature

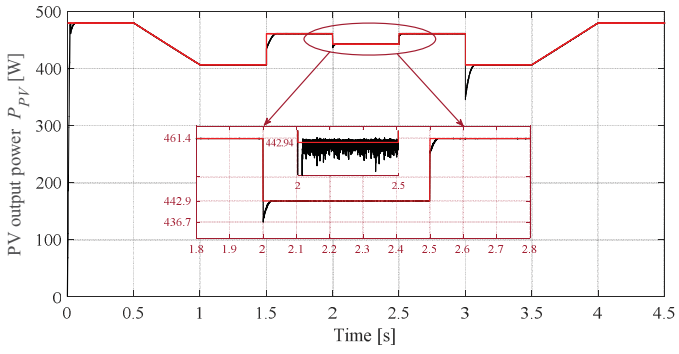

Fig. 9. Power of ***PV*** array for different levels of temperature .

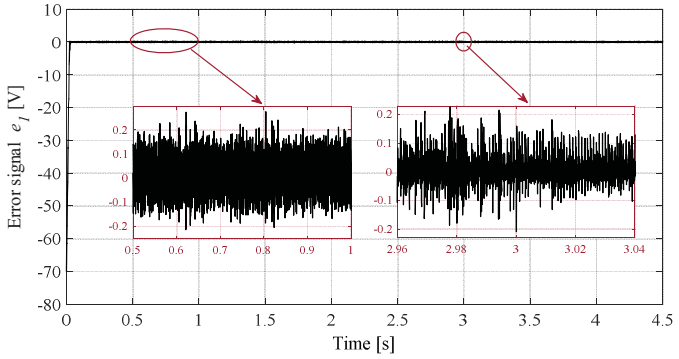

Fig. 10. Error signal e_1 under varying temperature .

V. COMPARISON WITH PI AND SMC CONTROLLER

To show the performance of the ***BSC***, it is compared with ***SMC*** and ***PI*** controllers. These latter are simulated and compared with the same conditions (sampling time and PWM frequency) at varying temperature and irradiance levels.

A. Comparison under varying irradiance

Figs. 11, 12 and 9 shows respectively the simulated of PV voltage, PV power and error signal with conventional ***PI*** and ***SMC*** controllers. First of all, the irradiation level is fixed at 400 W/m². The V_{PV} voltage with conventional ***PI*** and ***SMC*** methods is fluctuating around the reference ***Vref*** between (65.41-64.64V) and (65.53-65V) respectively.

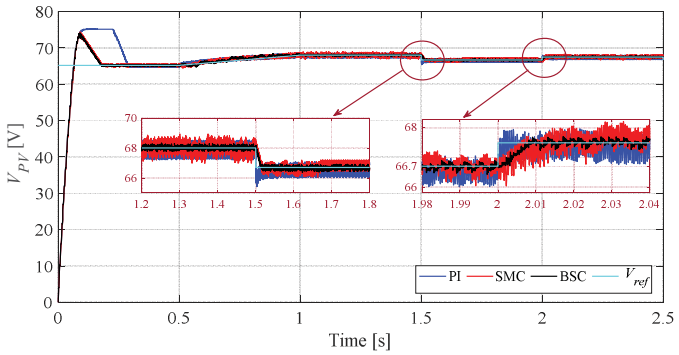

Fig. 11. Backstepping vs ***PI*** and ***SMC*** tracking of V_{PV}

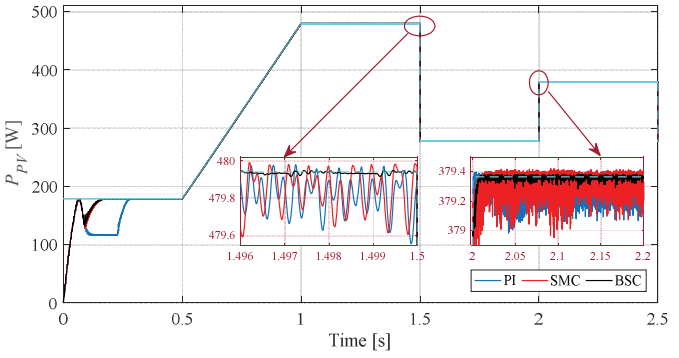

Fig. 12. Backstepping vs ***PI*** and ***SMC*** power of PV array under variation irradiance

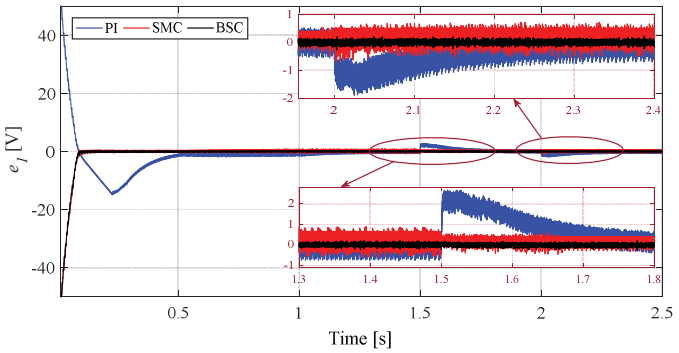

Fig. 13. Backstepping vs ***PI*** and ***SMC*** error signal under varying irradiance.

Moreover, for the proposed ***BSC***, the PV voltage tracks accurately its reference with fewer voltage fluctuations between (65.35- 65.02V).

On the other hand, it can be seen that not only the *BSC* reaches the MPP more rapidly than the PI and ***SMC***, but during the variation of irradiance level at 0.5; 1.5; 2 seconds, the backstepping controller displays superior performance in terms of maximum overshoot, response time and minimal oscillations compared to the other methods.

B. Comparison under varying temperature

In this 2nd comparison test, all the regulators are tested done below varying temperature levels. The irradiance is set at 1000 W/m² and temperature firstly is stepped up gradually from T= 25 °C to T = 65 °C at 1 seconds, and suddenly stepped down and up from tow steps T=65 °C to 35 at 1.5 seconds and from 35 °C to 45 °C at 2 seconds.

The obtained results are illustrated in Figs. 14, 15 and 16. It can be seen that the waveforms of V_{PV} and P_{PV} are reverse proportional to the change of temperature.

The PV voltage with conventional ***PI*** and ***SMC*** methods is fluctuating around the reference ***Vref*** between (58.54-57.4V) and (58.53-57.42V) respectively, in other hand, it can be seen that ***BSC*** reaches our system in a minimal time with fewer oscillations between (58.22-57.99) as compared to ***PI*** and ***SMC*** controllers. On the same figures a zoomed view of the fluctuations about the MPP of all controllers.

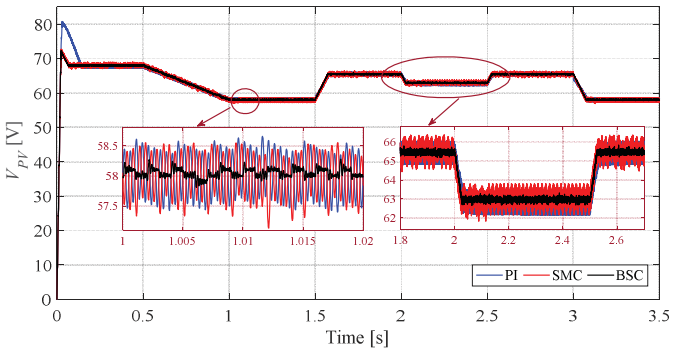

Fig. 14. Backstepping vs ***PI*** and ***SMC*** Tracking of V_{PV}

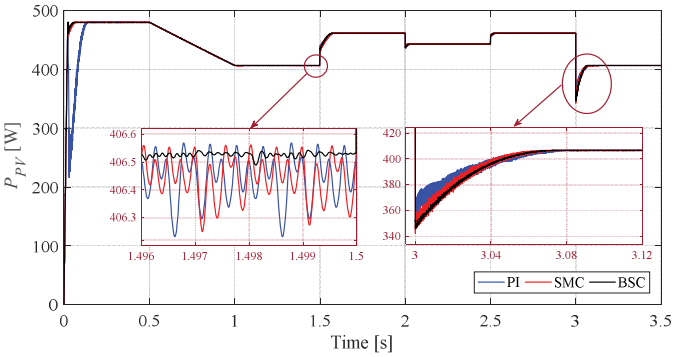

Fig. 15. Bachsteppng vs ***PI*** and ***SMC*** power of PV array under variation temperature

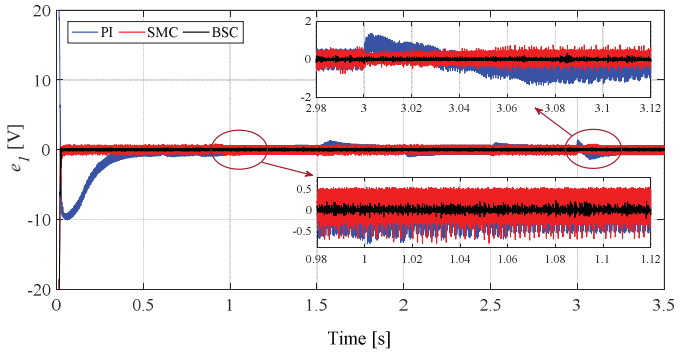

Fig. 16. Backstepping vs ***PI*** and ***SMC*** error signal under varying temperature

VI. CONCLUSION

In this paper, robust and nonlinear backstepping has been applied to track the maximum power point MPP of a photovoltaic system .

The PV generator is to the load (resistance) via through a DC-DC boost power converter.

The PV generator is is linked to the load (resistor) via a DC-DC boost power converter. To get maximum power P_{mpp} from photovoltaic array, the duty cycle μ of the boost chopper is controlled through which the PV array output voltage is tracked to the voltage reference , this latter has been generated by the P&O method.

The verification of the asymptotic stability of photovoltaic chain is performed via Lyapunov stability analysis. The simulation results show that the controller *BSC* verified and performed well below the sudden and gradual variation of climatic conditions, which prove the good robustness of the *BSC* proposed controller.

The comparison with the traditional technic used in the past P&O/PI and SMC/PI controllers are made which shows that the *BSC* performed better and most efficiently during the variation in the climatic conditions (irradiance & temperature levels).

As a future perspective, an implementation of the proposed controller using a dSPACE system be introduced.

REFERENCES

[1] A. Bahadori, C. Nwaoha, S. Zendehboudi, et G. Zahedi, « An overview of renewable energy potential and utilisation inAustralia », Renew. Sustain. Energy Rev., vol. 21, p. 582□589, mai 2013.

[2] P. A. Owusu et S. Asumadu-Sarkodie, « A review of renewable energy sources, sustainability issues and climate change mitigation », Cogent Eng., vol. 3, no 1, p. 1167990, 2016.

[3] T.-F. Wu et Y.-K. Chen, « Modeling PWM DC/DC converters out of basic converter units », IEEE Trans. Power Electron., vol. 13, no 5, p. 870–881, 1998.

[4] H. El Fadil et F. Giri, « Backstepping based control of PWM DC-DC boost power converters », in Industrial Electronics, 2007. ISIE 2007. IEEE International Symposium on, 2007, p. 395–400.

[5] M. G. Villalva et E. Ruppert, « Analysis and simulation of the P&O MPPT algorithm using a linearized PV array model », in Industrial Electronics, 2009. IECON'09. 35th Annual Conference of IEEE, 2009, p. 231–236.

[6] S. K. Kollimalla et M. K. Mishra, « A new adaptive P&O MPPT algorithm based on FSCC method for photovoltaic system », in 2013 International Conference on Circuits, Power and Computing Technologies (ICCPCT), 2013, p. 406–411.

[7] K. Ishaque, Z. Salam, et G. Lauss, « The performance of perturb and observe and incremental conductance maximum power point tracking method under dynamic weather conditions », Appl. Energy, vol. 119, p. 228–236, 2014.

[8] A. Morales-Acevedo, J. L. Diaz-Bernabe, et R. Garrido-Moctezuma, « Improved MPPT adaptive incremental conductance algorithm », in IECON 2014-40th Annual Conference of the IEEE Industrial Electronics Society, 2014, p. 5540–5545.

[9] A. Laib, F. Krim, B. Talbi, A. Kihal, et A. Sahli, "Predictive Control Strategy for Double-Stage Grid Connected PV Systems," in *Advanced Control Engineering Methods in Electrical Engineering Systems,* 2019, p. 314-327.

[10] A. Laib, F. Krim, B. Talbi, A. Kihal, et H. Feroura, "Improved Control for Three Phase dual-Stage Grid-Connected PV Systems Based on Predictive Control Strategy," *J. Control Eng. Appl. Inform.,* vol. 20, nº 3, p. 12-23-23, sept. 2018.

[11] B. Talbi, F. Krim, T. Rekioua, A. Laib, et H. Feroura, "Design and hardware validation of modified P&O algorithm by fuzzy logic approach based on model predictive control for MPPT of PV systems," *J. Renew. Sustain. Energy*, vol. 9, nº 4, p. 043503, juill. 2017.

[12] E. Bianconi et al., « Perturb and observe MPPT algorithm with a current controller based on the sliding mode », Int. J. Electr. Power Energy Syst., vol. 44, no 1, p. 346–356, 2013.

[13] A. Belkaid, J. P. Gaubert, et A. Gherbi, « An improved sliding mode control for maximum power point tracking in photovoltaic systems », J. Control Eng. Appl. Inform., vol. 18, no 1, p. 86–94, 2016.

[14] A. Kihal, F. Krim, B. Talbi, A. Laib, et A. Sahli, "A Robust Control of Two-Stage Grid-Tied PV Systems Employing Integral Sliding Mode Theory," *Energies*, vol. 11, nº 10, p. 2791, oct. 2018.

[15] A. Kihal, F. Krim, A. Laib, B. Talbi, et H. Afghoul, " An improved MPPT scheme employing adaptive integral derivative sliding mode control for photovoltaic systems under fast irradiation changes," *ISA Trans.*, vol. 87, p. 297-306, avr. 2019.

[16] W. Dazhong et W. Xiaowei, « A photovoltaic MPPT fuzzy controlling algorithm [J] », Acta Energiae Solaris Sin., vol. 6, p. 008, 2011.

[17] B. N. Alajmi, K. H. Ahmed, S. J. Finney, et B. W. Williams, « Fuzzy-logic-control approach of a modified hill-climbing method for maximum power point in microgrid standalone photovoltaic system », IEEE Trans. Power Electron., vol. 26, no 4, p. 1022–1030, 2011.

[18] S. Lalouni et D. Rekioua, « Modeling and simulation of a photovoltaic system using fuzzy logic controller », in Developments in eSystems Engineering (DESE), 2009 Second International Conference on, 2009, p. 23–28.

[19] H. K. Khalil et J. W. Grizzle, Nonlinear systems, vol. 3. Prentice hall Upper Saddle River, NJ, 2002.

[20] N. H. McClamroch, « Stability of Dynamical Systems-On the Role of Monotonic and Non-Monotonic Lyapunov Functions [Bookshelf] », IEEE Control Syst. Mag., vol. 36, no 1, p. 77–78, 2016.